ORNL/TM-2018/895

Summary of RF Technology Program Activities
October 2013 – September 2017

R. H. Goulding
E. H. Martin
G. L. Bell
J. B. O. Caughman

June 26, 2018

Support of National RF Research and Development Field Work Proposal ERAT560

G. L. Bell, Principal Investigator

Barry Sullivan, Federal Program Manager
Office of Fusion Energy Sciences

OAK RIDGE NATIONAL LABORATORY
MANAGED BY UT-BATTELLE FOR THE US DEPARTMENT OF ENERGY

ORNL/TM-2018/895

Fusion and Materials for Nuclear Systems

SUMMARY OF RF TECHNOLOGY PROGRAM ACTIVITIES

R. H. Goulding
E. H. Martin
G. L. Bell
J. B. O. Caughman

Date Published: June 18, 2018

Prepared by
OAK RIDGE NATIONAL LABORATORY
Oak Ridge, TN 37831-6283
managed by
UT-BATTELLE, LLC
for the
US DEPARTMENT OF ENERGY
under contract DE-AC05-00OR22725

CONTENTS

LIST OF FIGURES

LIST OF FIGURES (CONT'D)

ACRONYMS

APS	American Physical Society
DC	Direct Current
DFSS	Dopler Free Saturation Spectroscopy
DIII-D	DIII-D National Fusion Facility
EBW	Electron Bernstein Wave
EC	Electron Cyclotron
ECH	Electron Cyclotron Heating
ECR	Electron-cyclotron Resonant
ELM	Edge Localized Mode
FMIT	Fusion Materials Irradiation Test
FMNSD	Fusion and Materials for Nuclear Systems
FRT	Fixed Radio Transmitter
ICH	Ion Cyclotron Heating
ICRF	Ion Cyclotron Range of Frequencies
IEDF	Ion Energy Distribution Function
JET	Joint European Torus
LH	Lower Hybrid
MPEX	Material Plasma Exposure eXperiment
NFM	Nuclear Fuels and Materials Group
NRRDP	National RF Research and Development Program
OES	Optical Emission Spectroscopy
Proto-MPEX	Proto-Material Plasma Exposure eXperiment
RF	Radio Frequency
R&D	Research and Development
SRA	Spoke Ring Assembly
UCSD	University of California at San Diego
VSWR	Voltage Standing Wave Ratio
WEST	'W' Environment in a Steady-state Tokamak

ABSTRACT

The goals of the National RF Research and Development Program (NRRDP) are to advance the basic understanding of high power radio frequency (RF) in a plasma environment, and to maintain the high-power transmitters and cooling water systems required to support the ITER Ion Cylcotron Range of Frequencies (ICRF) transmission line high power component testing and operation of the Proto-Material Plasma Exposure eXperiment (MPEX) device. The work includes the study of the RF sheath, and development of RF-related diagnostics. These include active and passive spectroscopic diagnostics that can provide local and line integrated measurements of RF and Direct Current (DC) electric fields in the edge plasma of fusion devices, as well as measurements of other parameters.

One of these, the Doppler Free Saturation Spectroscopy (DFSS) diagnostic, utilizes a laser beam split into two intersecting, counter-propagating pump and probe beams, whose intersection defines the measurement region. DFSS has demonstrated measurements of atomic spectra with 500 times greater resolution than passive Optical Emission Spectroscopy (OES). This allows Stark effect based electric field measurements to be made with two orders of magnitude high sensitivity than with OES. Measurements have been made using an ORNL electron-cyclotron resonant (ECR) plasma source producing densities up to 10^{19} m-3, in the vicinity of an RF-biased planar electrode.

In addition, highly accurate measurement of background magnetic fields via Zeeman splitting has been demonstrated in the device, and studies are underway to apply the technique to plasma density measurements in order to obtain more precise edge plasma density profiles.

OES has been applied to the measurement of RF electric fields near the plasma facing surface of a lower hybrid launcher on the Alcator C-Mod tokamak. A strong poloidal field component was observed experimentally that was not initially reproduced in a COMSOL full-wave plasma model. It was found that incorporating realistic turbulence-induced density fluctuations produced a polarization angle that more closely matched the experimental measurements. Similar experiments are planned on 'W' Environment in a Steady-state Tokamak (WEST). In addition, a proof-of-principle Proto measurement has been made of $D_{\square}$ emission modulated by an electron cyclotron heating (ECH) generated electric field in the external plasma on the DIII-D National Fusion Facility (DIII-D), in which harmonics of the ECH frequency are observed that can be related to the electric field magnitude. The technique will be used to improve understanding of beam defocusing, mode conversion, and scattering by turbulence.

Work was initiated to investigate electrostatic coupling and sheath formation in the near field of a RF driving/DC grounded electrode simulating the capacitive coupling between surfaces that have a non-zero RF impedance to ground and the edge plasma. A retarding field energy analyzer was placed downstream of the sheath to measure the ion energies on field lines mapped to the electrode. Initial measurements indicate an increase in ion energies as the RF electrode voltage increased. The practical impact is that higher energies will lead to increased erosion of surfaces magnetically connected to the plasma and thereby introduce impurities into the plasma.

Much of the work at the ORNL Multi-Purpose High-Bay Facility at ORNL, though funded by other programs, depends on high power RF sources maintained by the NRRDP. This includes high power tests of component designs for the ITER Ion Cyclotron Transmission Line and Matching System, and operation of the fully RF powered Prototype Material-Plasma Exposure eXperiment (Proto-MPEX) ITER transmission line component test articles including straight sections, elbows, gas barriers, assembly bellows, a power splitter, and coaxial switch have been tested for power, voltage, and current handling at levels at or above those specified for ITER. Steady state power handling of 6 MW and short pulse voltage handling up to ~ 100 kV have been demonstrated for some components.

Also utilizing NRRDP supported RF and microwave sources, Proto-MPEX has produced deuterium plasma densities up to 8×10^{19} m^{-3}, surpassing the design specification. Ion heating in the core plasma by the ion cyclotron heating (ICH) system has been demonstrated at high density (3.5×10^{19} m^{-3}), and overdense electron Bernstein wave (EBW) heating has been achieved, increasing the electron temperature to > 20 eV.

1. BUDGET SUMMARY AND JUSTIFICATION

This program provides resources to advance the basic understanding of high power RF in a plasma environment, maintain the high-power transmitters and cooling water system required to support ITER ICRF transmission line high power component testing and operation of the Proto-MPEX device, and develop a Doppler Free Saturation Spectroscopy diagnostic with the aim to measure the local electric field distribution in the near field region of RF antennas.

Table 1 summarizes the RF Technology Program costs for the reporting period, FY2014-2017. The labor cost comprises wage pool and organizational burden. Labor costs include support for researchers, engineers, technical professionals, postdoctoral research associates, technicians, and administrative support. Materials purchases include fabrication materials, vacuum hardware, vacuum pumps, pressure gauges, oscilloscopes, network analyzers, optical components, lasers, RF sensors, gases, LabView licenses, MatLab licenses, data acquisition and control hardware and software, etc. needed to execute the mission. Subcontracting costs cover students. Internal services cover occasional graphics and technical editing support. Laboratory overhead is listed explicitly. No major equipment procurements were made during the performance period.

Key objectives and achievements for the reporting period are shown in Table 2

Table 1. Summary of RF Technology Program Costs for FY0214-2017

Category	FY2014	FY2015	FY2016	FY2017	Total
New Budget Authority	$500,000	$500,000	$500,000	$500,000	$2,000,000
Labor	$348,452	$337,217	$125,688	$340,488	$1,151,844
Materials	$113,605	$95,694	$60,174	$61,362	$330,835
Subcontracts	$39,460	$34,239	$42,411	$27,632	$143,741
Travel	$11,280	$25,635	$8,826	$10,327	$56,069
Internal Services	$1,086.47	$846.00	$9.20	$3,179.00	$5,121
Laboratory Overhead	$136,400	$139,737	51,574	$135,217	$462,928
Total Cost	$650,285	$633,367	$288,682	$578,204	$2,150,538

Note: FY2013 carryover = $354,657

Table 2. Key objectives and achievements for Fiscal Years 2014-2017

Key Objective	Achievement	Fiscal Year
Complete repairs to Fusion Materials Irradiation Test (FMIT) transmitter	Repairs to relays in interlock chain completed 10/13. Line stretchers repaired 7-8/14.	2014
Complete assembly of SPA antenna	Plating of the current strap was completed and the antenna was assembled in the summer of 2014.	
Complete repairs of the Fixed Radio Transmitter (FRT)-86 transmitter and test into dummy load	Replacement of HV power supply contactors 10/14, Replacement of vacuum capacitors in Power Amplifier output tank circuit 11/14, 480 VAC arc damage related repairs completed 3/15, Air cooling system rebuild completed 3/15.	2015
Complete installation of Doppler-Free Saturation Diagnostic on small experiment and initiate shakedown	Advanced Plasma Source Test Stand was assembled and commissioned 3/16. Installation of DFSS was completed and first measurements acquired 7/16.	2016
Maintain operational status of FMIT, FRT-85, and FRT-86 transmitters to enable successful execution of ITER high power RF transmission line component testing and operation of Proto-MPEX	FMIT maintenance done on Final Power Amplifier/driver fused disconnect switch and transformer/rectifier unit in March/April 2016. FRT-85 and 86 maintained in operational status	
Maintain operational status of FMIT, FRT-85, and FRT-86 transmitters to enable successful execution of ITER high power RF transmission line component testing and operation of Proto-MPEX	Miscellaneous repairs done to FMIT, FRT-85 and FRT-86 to maintain operational status. Sairem RF generator added 9/17.	2017

2. PROGRAM SUMMARY

The goals of the National RF Research and Development Program are to advance the basic understanding of high power RF in a plasma environment and to maintain the high-power transmitters and cooling water systems required to support the ITER ICRF transmission line high power component testing and operation of the Proto-MPEX device. In this section we first discuss development of active and passive spectroscopically based diagnostics used to measure electric fields near RF launching structures. We also discuss RF sheath interaction studies that have been conducted as part of this program, and finally give an overview of the research that has been accomplished utilizing the high-power RF sources maintained under this program, as well as list the specific maintenance and repair activities occurring during the review period.

2.1 DOPPLER-FREE SATURATION SPECTROSCOPY AT ORNL

A significant effort has been made over the last three years to develop a diagnostic capable of measuring the local plasma density, electric field vector, and magnetic field vector in the edge plasma of magnetic fusion energy devices. The purpose is to provide high resolution experimental data that can be used to validate theoretical models and exascale relevant computational simulations of RF heating and current

drive systems. The diagnostic implements DFSS to measure the spectral line profile. which is then fit to a quantum mechanical model to extract the plasma density and electric/magnetic field vectors. This work consisted of: (1) a major upgrade of existing experimental test-stand, (2) design of a DFSS system and procurement of optics and laser, (3) assembly and implementation of the DFSS system, (4) development of spectroscopic fitting software, and (5) initial DFSS magnetic field measurements.

DFSS is a laser-based technique in which the line profile can be measured with unprecedented spectral resolution, enabling simultaneous measurement of the local plasma density, electric field vector, and magnetic field vector. Typically, electric and magnetic field vectors have been measured with passive OES [1-3]. This technique requires large magnitude fields, approximately 1,000 V/cm and 10,000 Gauss respectively, and is based on observing emission naturally occurring within the plasma yielding a 2D line of sight measurement. Implementing DFSS yields a local 3D measurement and can increase the resolution limits by 2 to 3 orders of magnitude, to approximately 10 V/cm and 10 Gauss.

In order to develop a DFSS system relevant for the edge plasma of a magnetic fusion energy device, a sufficiently high density of 5-10 x 10^{18} m^{-3} is required. ORNL's previous experimental test-stand was upgraded to produce electron densities (n_e) in this range, with three magnet coils added, and the power of the microwave generator increased from 300 to 1500 W. Figure 1 depicts a CAD cross-section of the upgraded test-stand and an image of the device in operation.

An RF electrode was designed to study the magnetized RF sheath relevant to ICRF antennas. Figure 2 presents an image of the RF electrode after assembly and in operation; the RF sheath is visible by the pink glow presented in Figure 2b. Future work will be focused on experimental measurements of the magnetized RF sheath electric field using this electrode and DFSS. These measurements will allow for direct validation of a novel RF sheath boundary condition [4]. Once validated, the RF sheath boundary condition will be used to model ICRF antennas self consistently. ORNL's DFSS system was designed to yield a 300x increase in resolution when compared to passive OES techniques [5]. At this resolution the plasma density has a sufficiently large effect on the spectrum and can be characterized [6]. The use of DFSS as a plasma density diagnostic is the focus of a Ph.D. student, Abdullah Zafar (North Carolina State University), who is working onsite at ORNL. Abdullah's dissertation work is in its final stages and will outline the applicability of the quasi-static approximation for Stark broadening at low plasma density.

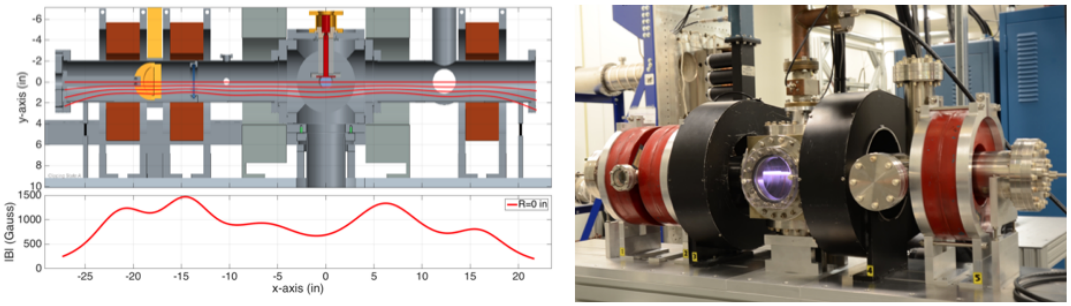

(a) **(b)**

Fig. 1. (a) CAD drawing of upgraded experimental test stand, magnetic field lines are shown in red. The magnetic field magnitude on axis is plotted as a function of position in the device. (b) Image of experimental test-stand in operation.

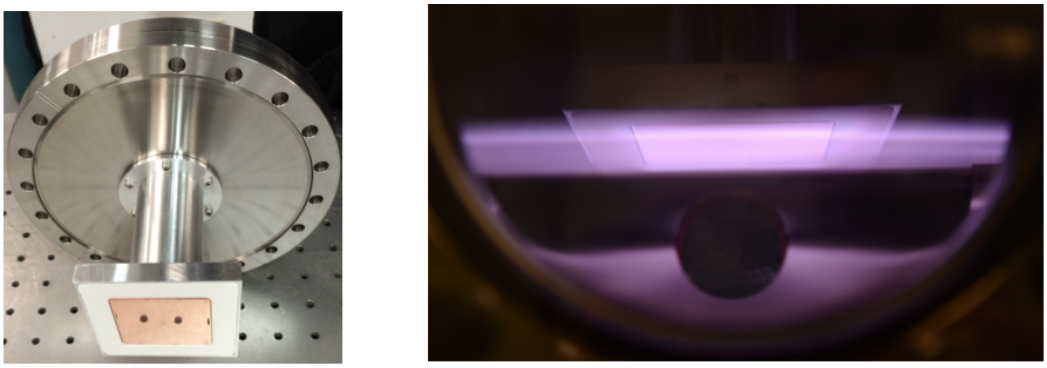

(a) (b)

Fig. 2. (a) Image of the RF electrode after assembly and (b) in operation. The RF sheath is visible by the light pink optical emission. A 13.56 MHz RF power supply was used outputting 300 W of power.

DFSS can be summarized in three steps [5]. First, two laser beams are generated from a single source. These are referred to as the probe and pump beams. Second, they are aligned such that they are counter-propagating at a small angle ($\theta<3°$) and intersect at the desired measurement location. Third, the probe beam transmission intensity is measured as the laser frequency is swept over that associated with the atomic transition of interest. Figure 3a presents an example of an H_α Doppler-free spectrum obtained with ORNL's DFSS system (red) and the associated spectrum that would be measured using passive OES (black). The electric and magnetic field associated with these spectra are 0 V/cm and 875 Gauss, respectively. The detailed structure present in the DFSS spectrum (red) is due to Zeeman splitting by the magnetic field. The resolution increase was determined to be approximately x500, significantly exceeding the design specification. These spectra were obtained on the upgraded experimental test-stand depicted in Figure 1. Figure 3b presents a simple cartoon of the DFSS setup, indicating the counter propagating laser beam geometry associated with the diagnostic. The location of the DFSS measurement is determined by the overlap of the pump and probe laser beams, indicated by the black marker of Figure 3b. Photographs of the pump and probe beam optics are shown in Figure 4.

The DFSS system is currently being used to conduct its first round of high-fidelity experiments to measure the well characterized magnetic field of the upgraded test-stand shown in Figure 1. A He-I transition is being measured instead of H_α because it has a much simpler Zeeman splitting profile. To extract the magnetic field from Doppler-free spectra a new software package, sFIT, was written. This software implements a robust optimization routine using a previously developed quantum mechanical based model called the Explicit Zeeman Stark Spectral Simulator [7]. Figure 5a presents the measured and actual magnetic field as a function of the magnetic field coil current of the black coils shown in Figure 1b. The measured magnetic field was determined by fitting the He-I Doppler-free spectra to sFIT. Figure 5b presents the experimental data (markers) and the fit (line) for two different magnetic field intensities generated by a magnetic field coil current of 120 (blue) and 195 (black) amps. The two extreme peaks of Figure 5b are the result of Zeeman splitting. The actual magnetic was measured by a recently calibrated magnetic field meter and is known with an error of ± 3 Gauss. It was found that the DFSS based magnetic field measurements coincided with the actual values within ± 7 Gauss, as indicated by Figure 5a.

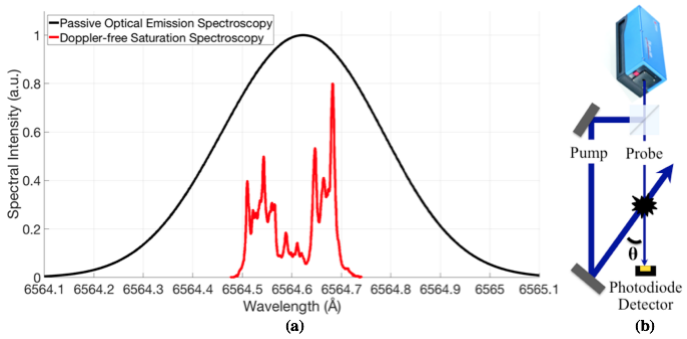

Fig. 3. H_α (a) Passive OES spectrum (black) and DFSS spectrum (red) measured under 0 V/cm and 875 Gauss. The structure present in the DFSS spectrum is due to Zeeman splitting. (b) Simple cartoon of the DFSS setup. The location of the measurement is determined by the overlap of the pump and probe laser beams, indicated by the black marker.

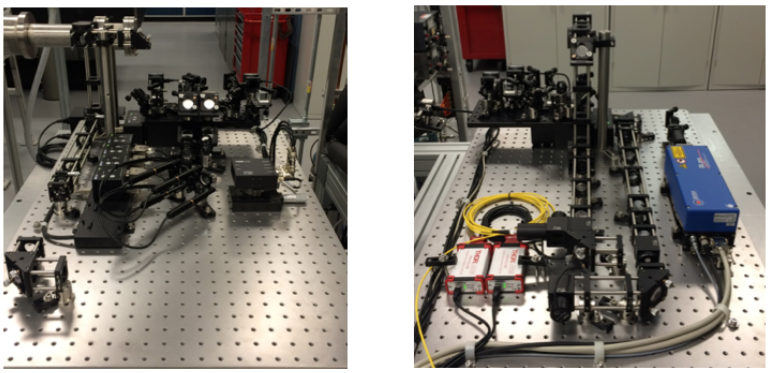

Fig. 4. DFSS optics associated with the (a) pump and (b) probe beams. These optical tables are positioned on either side of the experimental test-stand shown in Figure 1.

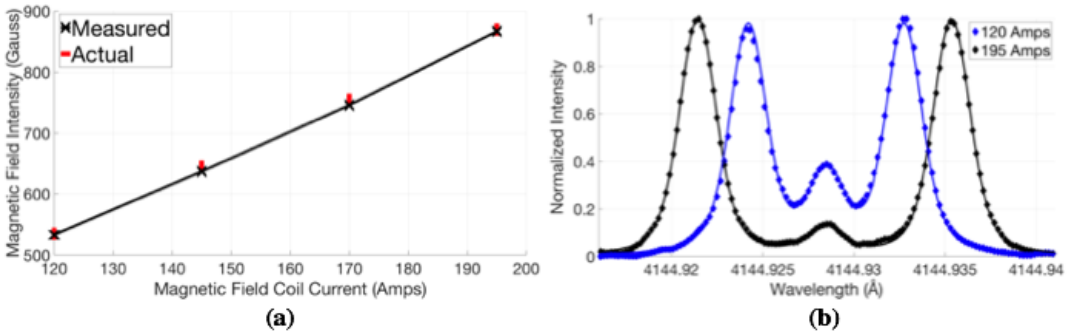

Fig. 5. (a) DFSS based magnetic field measurements as a function of magnetic field coil current. The actual magnetic field was measured by a meter and has an error of ± 3 Gauss. (b) DFSS obtained He-I spectral data (makers) and sFIT results (line) for two magnetic field intensities.

2.2 LOWER HYBRID WAVE ELECTRICAL FIELD MESUREMENTS ON ALCATOR C-MOD

New experimental measurements of the Lower Hybrid (LH) wave electric field vector, $\overline{E}_{LH}$, in Alcator C-Mod were obtained, and provided a direct comparison with 3D full-wave COMSOL simulations using the cold plasma dielectric tensor and reflectometry measured density profiles. Two key results were found: 1) The direction of $\overline{E}_{LH}$ was found to have a substantial poloidal component, in strong disagreement with the nearly radial full-wave simulation result and 2) Adding Scrape Off Layer (SOL) density fluctuations [8,9] to the density profile implemented in the full-wave simulations can be used to explain the $\overline{E}_{LH}$ direction discrepancy.

Polarized passive OES was implemented to measure two orthogonally polarized D_β spectra. The spectral line profiles were simultaneously fit to the Schrodinger equation containing both magnetic and time periodic electric field operators [2,7] using sFIT to extract the three components of $\overline{E}_{LH}$. The experimental $\overline{E}_{LH}$ results were compared to 3D full-wave COMSOL simulations via a synthetic diagnostic. Figure 6 shows the COMSOL results for $|\overline{E}_{LH}|$ at a power of 330 kW and a line averaged density of 1.3 x 10^{20} m^{-3}. An image of the LH launcher showing the magnetic field aligned measurement locations as red circles is superimposed, with presented data highlighted in white. Comparing the experimental and simulation results, good agreement was found with regard to the magnitude of $\overline{E}_{LH}$ both as a function of measurement location and LH power. However, it was found experimentally that $\overline{E}_{LH}$ contained a poloidal component having a magnitude comparable to or greater than that of the radial component. This was found to be a strong function of tokamak poloidal angle, increasing towards the midplane, and a weak function of toroidal angle, remaining approximately constant in that direction. In contrast, the simulations predict a nearly radial direction for $\overline{E}_{LH}$. Figure 7 presents the direction of $\overline{E}_{LH}$ averaged over 200 to 400 kW of net LH power for the white highlighted vertical (right) and horizontal (left) locations of Figure 6. Varying the density profile in the simulation resulted in strong changes in the magnitude of $\overline{E}_{LH}$, but not the direction. However, adding SOL density fluctuations to the model based on a 3D BOUT turbulence simulation [9] produced diffraction and scattering generating a substantial poloidal component of $\overline{E}_{LH}$, yielding results much closer to the experimental measurements, as seen in the figure. This suggests that SOL turbulence can have a detrimental effect on lower hybrid current drive performance if the wavelength is on the order of the turbulence characteristic scale length. Reactor relevant scenarios are likely to experience enhanced turbulence in the SOL, further motivating the need to test innovative solutions such as the high field side launch lower hybrid scheme tentatively scheduled for installation on DIII-D. Similar measurements are planned for a WEST LH launcher during the C4 campaign. Wire grid polarizers have been fabricated for these measurements and tested at 300°C to ensure compatibility with WEST.

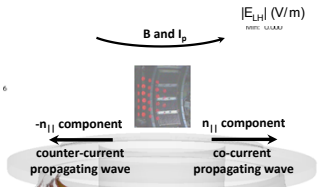

Fig. 6. 3D full-wave COMSOL simulation of $\overline{E}_{LH}$ for C-Mod discharge 1160818010. The measurement location of the presented data is highlighted in white.

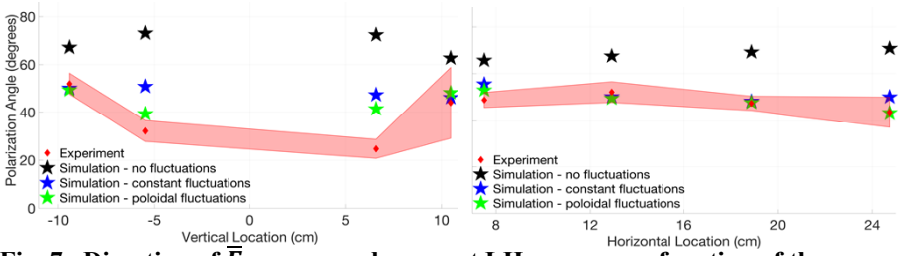

Fig. 7. Direction of $\overline{E}_{LH}$ averaged over net LH power as a function of the white highlighted vertical (left) and horizontal (right) locations of Figure 6. The coordinate system origin is centered about the LH launcher. At the midplane, the poloidal and radial directions correspond to 0 and 90 degrees, respectively.

2.3 ELECTRON CYCLOTRON WAVE ELECTRIC FIELD MEASUREMENTS ON DIII-D

High powered electron cyclotron (EC) waves are widely used for heating, current drive, and control in current magnetic fusion experiments such as DIII-D [11], TCV [12], ASDEX-U [13], and W7-X [14]. In larger path length experiments such as ITER, there is likely to be more scattered power from turbulence, cross polarization from mode conversion, and defocusing of the EC beam. These effects can increase the power necessary to stabilize neoclassical tearing modes and increase the likelihood of stray microwave radiation damaging vacuum vessel components and diagnostics.

To further studies on the EC beam width and to explore other issues such as cross-polarization, a direct measurement of the EC wave amplitude, direction, and beam width in the scrape off layer plasma is highly desirable. We have conducted a proof of principal experiment whose purpose was to measure the D_β spectrum using passive OES and show the effect of the EC wave electric field. The EC wave electric field produces a series of satellites in the spectrum spaced about integer multiples of the wave frequency (110 GHz for DIII-D) [7]. Figure 8 presents a Fourier transform of time averaged D_β spectral data obtained during our proof of principal experiment at DIII-D. At low frequency, ~50 GHz, the Zeeman splitting is observed. At higher frequency, around 110 GHz and its harmonics, a satellite structure is present and is expected to be caused by the EC wave electric field.

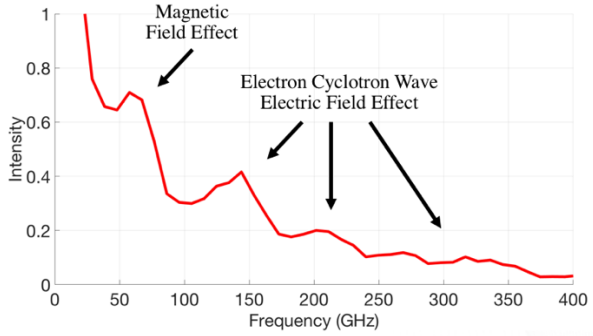

Fig. 8. Fourier transform of time averaged D_β spectral data obtained during our proof of principal experiment at DIII-D. Around 110 GHz and its harmonics, a satellite structure is present and is expected to be caused by the EC wave electric field.

2.4 PROTO-MPEX

Future work will consist of obtaining higher quality data during the remainder of the current DIII-D experimental campaign and the design of a diagnostics that would be capable of acquiring 2D spatial resolved EC beam images.

2.4.1 Background

Proto-MPEX (Prototype Material Plasma Exposure eXperiment) is a prototype linear device powered solely by RF for the study of plasma-materials interactions [14,15]. It is being used to develop the physics understanding necessary to design MPEX [16], which will be capable of generating high heat (> 10 MW/m^2) and particle (up to 10^{24}/m^2-s) fluxes under steady state conditions relevant to fusion reactors such as ITER and the DEMOnstration Power Station. MPEX, like Proto-MPEX, utilizes separate RF and microwave systems for plasma production, electron heating, and ion heating, and will have the capability of simulating a wide range of phenomena. As an example, RF heated ions can reproduce the features of the magnetic pre-sheath occurring when a field line intercepts a divertor surface at an angle, something

that is not possible in most linear devices where ion energy is controlled by modifying the target substrate bias.

The Proto-MPEX device (Figure 9) produces plasma using a 13.56 MHz helicon source that has operated at power levels up to ~ 130 kW and produced deuterium (D) plasma densities up to 8×10^{19} m^{-3}, surpassing the design goal. It interfaces with an axially varying magnetic field, with maximum |B| > 1.5T downstream from the helicon. Careful tailoring of the magnetic field profiles, as well as gas injection location and timing were necessary to reach this plasma density [14,17].

Electrons are heated by EBW using a 28 GHz gyrotron. This provides power coupling under overdense conditions ($\omega_{pe} > \omega_{ce}$). The most heavily studied approach to date uses O-X-B mode conversion [18]. Source electron temperatures up to 21 eV have been observed under overdense conditions. This compares to a goal of 25 eV, and was achieved at lower density than ultimately required, while providing proof-of-principle. The Proto-MPEX results are the first successful demonstration of overdense electron heating via EBW in a linear device. Ions are heated in Proto-MPEX using ion cyclotron heating [19] in the frequency range 6-8.5 MHz. Slow waves are launched from a high field region with $\omega < \omega_{ci}$ into a region of decreasing |B| and are absorbed at the fundamental cyclotron resonance. - Source temperatures up to 16 eV have been measured, compared to the eventual goal of 25 eV, at densities up to ~ 3.5×10^{19} m^{-3}.

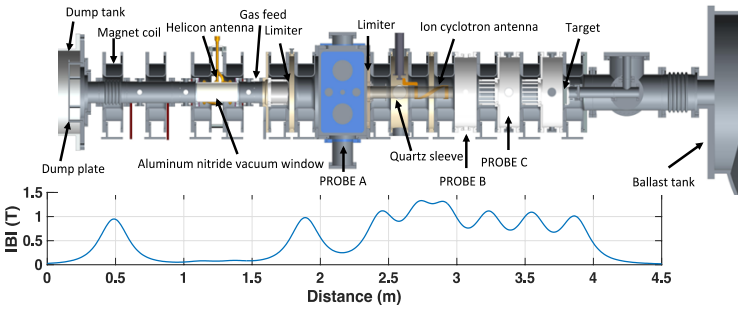

Fig. 9. Proto-MPEX Layout and axial magnetic field strength profile.

Progress on Proto-MPEX has been reviewed by an advisory committee consisting of participants from domestic and international laboratories, with reviews held in January for the past three years. The program achieved CD-0 status in March 2018.

2.4.2 Selected Results

An important milestone for Proto-MPEX was achieving ≥ 200 kW of injected RF power, a level that was reached in October 2017. Figure 10 shows the injected RF power in the milestone shot. Repairs and improvements to the FRT-86 transmitter supported by this program, and described in the next section, were critical to achieving this goal. Experiments in optimization of magnetic field and fueling geometry using RF power from the same transmitter ultimately led to production of true high-density helicon modes, achieved for the first time in April 2016 (Figure 11) [14], and subsequently modeled using COMSOL [17]. Figure 12 is a radial profile of n_e and T_e measured during an EBW heating experiment. It shows two points for which there is a 5-10 eV increase in the electron temperature at locations for which $n_e > 1.3 \times 10^{19}$ m^{-3} compared to a cutoff density of ~ 0.9×10^{19} m^{-3}. Finally, Figure 13 shows an increase in T_i observed during ion cyclotron heating experiments, determined by measurements of a Doppler broadened Ar II line in a plasma with ~ 10% Ar added to D. An increase of ~ 7 eV is seen when ICH is added for a chord passing through the axis, and when EBW heating is applied as well, an additional increase of 3 eV is seen. Figure 14 shows views of the ICH launcher. Initial ICH results are reported in Reference [19]. This work relied on the FRT-85 transmitter, also maintained by this program.

2.4.3 Status of Base-Program Goals and Tasks Related to Proto-MPEX

The main goal has been to "maintain the high-power transmitters and cooling water system required to support operation of the Proto-MPEX device." Achievement of this goal enables a robust experimental program. The transmitters include the 100 kW FRT-86 (steady-state) transmitter and the 20 kW (steady-state) FRT-85 transmitter, both of 1970s vintage, and the recently acquired Sairem 13.56 MHz fixed-frequency 100 kW RF generator, procured by the project as a replacement for the FRT-86, but with the FRT-86 retained to provide a backup and supplementary power.

A significant portion of the FRT-86 was refurbished during the first half of FY2015. This effort was completely supported by base program funding, and greatly increased the reliability of the transmitter. This work included

- Replacement of the high-voltage power supply contactors for the power amplifier tube and an associated resistor in the step-start circuit (October 2014),
- Replacement of two of the large vacuum capacitors in the power amplifier output tuning circuit, together with replacement of most of the internal water cooling lines (November 2014), Replacement of several smaller contactors and replacement of a distribution panel, after a 480VAC arc, as well as a condensate pump in the same timeframe (February-March 2015), and

A complete refurbishment of the forced air cooling unit including replacement of the impeller driveshaft and associated bearings (March 2015).

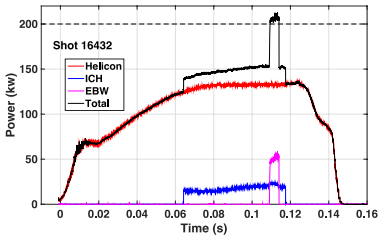

Fig. 10. Power traces for FRT-86 (helicon, red), FRT-85 (ICH, blue), and 28 GHz Gyrotron (EBW, magenta) for October 2017 milestone shot.

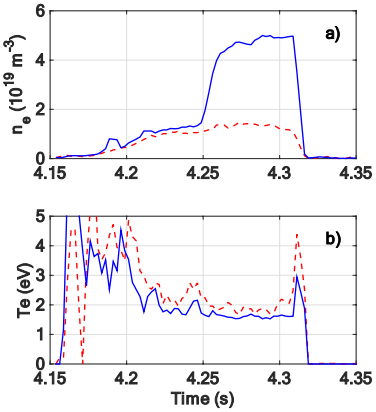

Fig. 11. Comparison of a) Plasma density, and b) electron temperature measured with double Langmuir probe with(solid blue lines) and without (dashed red lines) mode jump at "Probe C" location in Figure 9.

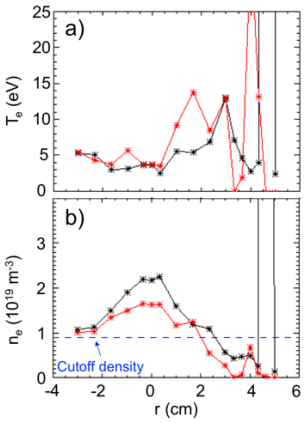

Fig. 12 a) Electron temperature and b) plasma density measured with (red lines) and without (black line) EBW heating by Thomson scattering at "Probe A" location in Figure 9.

Photographs of some of these components are shown in Figures 15 and 16. Other smaller modifications and repairs were made, including replacement of the socket for the driver tube (July 2016), and several times following failures of transistors and diodes on various control cards. These could take up to two days to troubleshoot and repair and occurred intermittently during the period of performance.

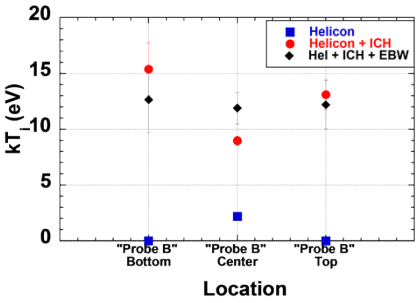

Fig. 13. Comparison of ion temperature measured with helicon alone, helicon+ICH, and helicon+ICH + EBW measured by Ar II line broadening.

a) b)

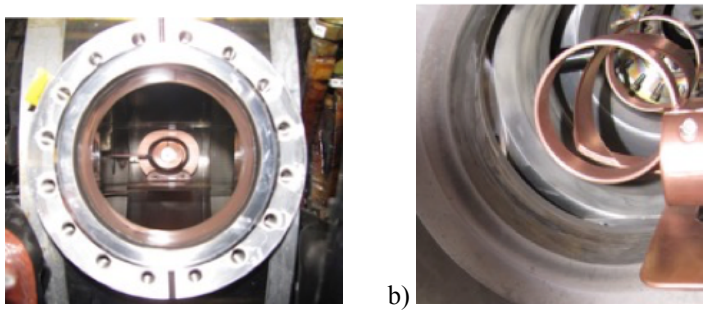

Fig. 14. a) View looking into ICH antenna vacuum feedthrough from opposite port, and b) view of antenna installed in chamber. There is a fused quartz tube that is surrounded by the antenna, which is removed in this view.

The FRT-85 transmitter used for ICH heating experiments encountered far fewer problems than the FRT-86. During the period of performance, there was one repair required in a low voltage power supply, several instances where the device was locked out to adjust internal tuning settings to change the operating frequency, and troubleshooting involving cathode overcurrent trips occurring during operation at frequencies below 7.5 MHz.

In addition to the work performed in the areas of maintenance and repair, operational support was also provided. This included work calibrating RF related diagnostics and operating and troubleshooting matching networks, etc.

2.4.4 Future Work

A network including coaxial switches and a power combiner has been designed and constructed to allow the output from the Sairem RF generator and the FRT-86 transmitter to be combined, producing up to 200 kW to power the helicon antenna (Figure 17). Based on previous results [14], it is likely that with this power increase, > $10^{20}m^{-3}$ density should be achievable in deuterium, and that it should be possible to increase the plasma diameter at the target as well. Funds from the RF Technology program are being used to design, construct, and test the control and protection system required to safely and successfully combine the power from the two RF sources. This added capability will be useful for other future applications, e.g. use on MPEX itself.

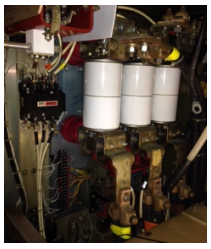

Fig. 15. FRT-86 HV power supply replacement vacuum contactors.

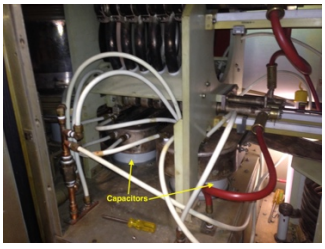

Fig. 16. FRT-86 Final Power Amplifier (FPA) output tuning circuit. Capacitors, white cooling water tubing, and red cooling water hoses were replaced.

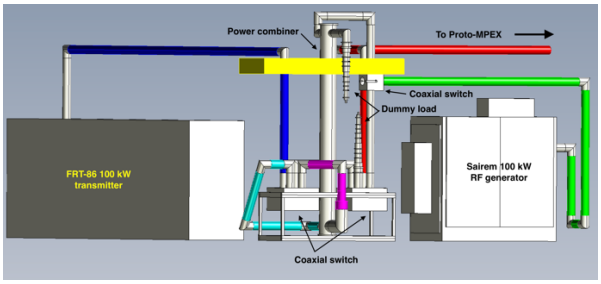

Fig. 17. Helicon 200 kW combiner network.

A collaboration has been established between ORNL and the University of California, San Diego (UCSD) to develop a steady-state water-cooled high power helicon window. A prototype is presently being fabricated and will be tested at UCSD on the Controlled Shear de-correlation Experiment helicon device at RF power levels up to 20 kW. Assuming the tests are successful, higher power testing will take place at a later date on Proto-MPEX. These tests will utilize the Sairem and FRT-86 RF sources supported by this program.

2.5 RF SHEATH INTERACTION MEASUSREMENTS

A powered RF electrode has been used to study RF sheath interactions in a magnetized plasma. The electrode was DC-grounded but RF driven to simulate the voltages that are formed on the surfaces of the antenna box that are in contact with the edge plasma. A picture of the electrode is shown in Fig. 2. The electrode was placed in a magnetized plasma (as shown in Fig. 1), and a retarding field energy analyzer was installed ~30 cm downstream of the electrode and used to measure the change in the ion energy distribution function (IEDF) on a magnetic field line connected to the electrode.

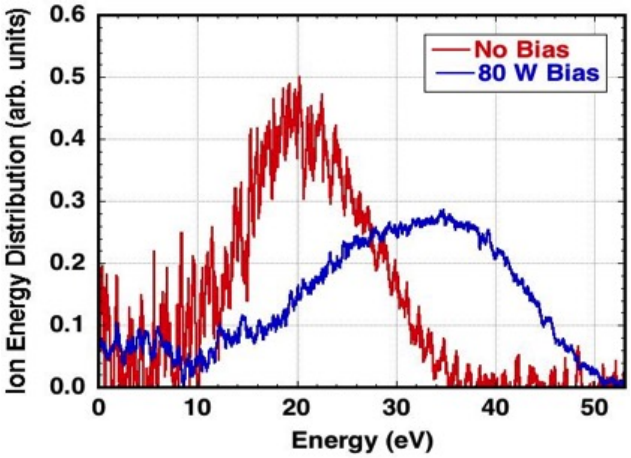

Fig. 18. The change in the IEDF on a magnetic field line connected to the powered electrode.

An example of the change in the IEDF with the presence of RF is shown in Fig. 18. The IEDF without any bias on the electrode shows a distribution which is consistent with an ECR plasma sheath with a 5 to 7 eV electron temperature. With the addition of a modest voltage on the upstream electrode (~95 V peak at 80 W), the IEDF significantly broadens and shifts to higher energies. The practical impact is that the higher ion energies will lead to increased erosion on surfaces that are magnetically connected to the antenna. Future experiments are planned by putting the electrode on a bellows drive and installing it on Proto-MPEX, which has field and plasma parameters that better simulate a tokamak edge plasma.

2.6 ITER ION CYCLOTRON TRANSMISSION LINE AND MATCHING SYSTEM

2.6.1 Background

The ITER Ion Cyclotron System operates over the frequency range 40-55 MHz and utilizes eight RF sources, each generating 3 MW @ Voltage Standing Wave Ratio (VSWR) ≤ 1.5. Power is fed to two ICH antennas through transmission lines of total length > 1 km. The 305 mm nominal outer diameter transmission lines are designed for a steady state upgrade power of 6 MW. Most have a 50 Ω characteristic impedance, while "unmatched" sections in the Port Cells have a 20 Ω characteristic impedance. To-date, tests have been performed only on the former type. For this type, pressurized N_2 gas flowing at velocities up to 5 m/s transfers heat generated at the center conductors and their supports to water cooled outer conductors. Additional requirements include the need to handle both internal and external pressure loads (internal pressures between 1000 Pa and 0.3 MPa absolute), and low per-component reflection (VSWR < 1.007). No commercially available components meet all the requirements, so new designs were developed by ORNL in collaboration with existing commercial transmission line suppliers.

High power RF tests are required in order to verify power handling. Test fixtures have been constructed at ORNL producing 6 MW of circulating RF power at low VSWR ≥ 1.05, and others producing high RF voltages and currents up to 100 kV peak and 1400 A rms respectively; the latter two values far exceed ITER requirements for components that have been tested. They operate steady state and include necessary gas pressurization and pumping capabilities. RF is supplied by a Fusion Materials Irradiation Test (FMIT) transmitter utilizing an EIMAC 8973 tetrode in the final power amplifier, and operates in the frequency range 40-80 MHz, with testing in frequency range 43-48 MHz. The transmitter has been upgraded to operate at up to 500 kW steady state, and has been used to test ITER transmission line components including straights and elbows, some of which use ORNL-developed spoke-ring-assembly (SRA) center conductor supports, assembly bellows used to facilitate installation of long runs of lines, also of the SRA type, three types of gas barriers, a hybrid power splitter, and a coaxial switch.

2.6.2 Selected Results

The SRA design was chosen for use on ITER based on mechanical and electrical tests results. Figure 19 is a photograph showing SRA. Figure 20 shows a series of high voltage tests an SRA straight section. It was subjected to four 3600 s long pulses at a voltage of 37 kV peak, with transients up to 42 kV peak, ~40% higher than the required value. In addition, the section withstood a maximum of 80 kV during 0.1s pulses without reaching a breakdown limit. High current tests were also run and currents up to 800 A peak were achieved for one-hour pulses, 33% greater than the required value.

Another example is testing performed on a hybrid power splitter (Figure 21). For these tests, it was necessary to develop a high-speed auto-tuning system that rapidly shifted the frequency in order to maintain the high Q resonance in the resonant line, of which the power splitter formed a part, as it underwent thermal expansion, as well as a system to rapidly re-apply power after arcs to prevent thermal de-tuning. Figures 22 and 23 show short pulse and long pulse voltages achieved for the power splitter, which are considerably higher than the required values (also shown).

2.6.3 Status of Base-Program Goals and Tasks Related to ITER Ion Cyclotron Testing

The main goal has been to "maintain the high-power transmitters and cooling water system required to support ITER ICRF high power transmission line component testing..." The FMIT transmitter was acquired in 1985. A considerable amount of work has been done during the period of performance in the areas of repair and maintenance. These included

- Replacement of relays and sockets in the device crowbar cabinet, as well as installing indicator lights to help with later troubleshooting of the interlock chain (October 2013)
- Replacement of the controller for the tuning stub in the FMIT single-stub matching network (December 2013)
- Troubleshooting of the Continental Dummy Load automatic temperature control (January 2014)
- Rebuilding two 9-inch diameter coaxial line stretchers (July – August 2014)

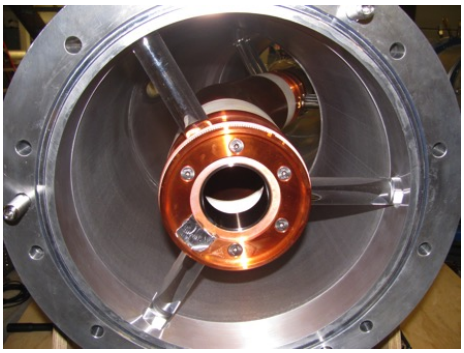

Fig. 19. SRA transmission line sections.

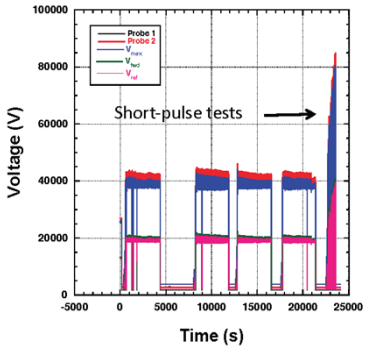

Fig. 20. Voltage vs. time for four 3600s pulses, followed by 0.1s pulses at voltages up to ~ 85 kV.

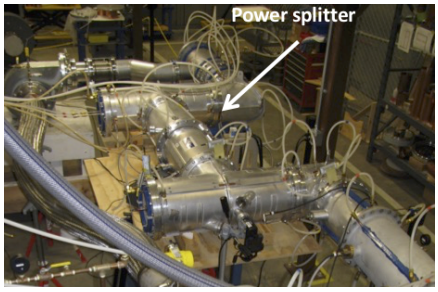

Fig. 21. 6 MW power splitter.

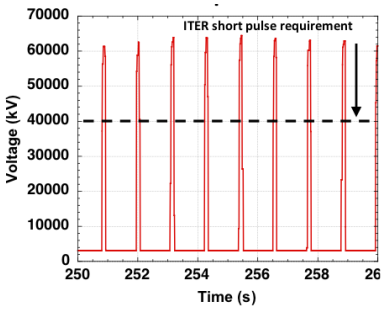

Fig. 22. Voltage vs. time for 0.1 s pulses.

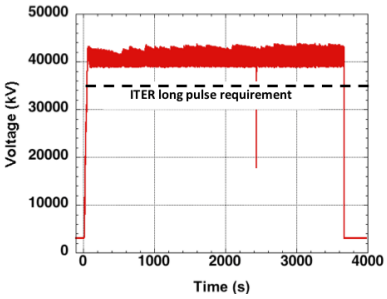

Fig. 23. Voltage vs. time for 3600 s pulse.

- Replacement of damaged FPA cavity tune/load drive rods, requiring cavity disassembly/reassembly (July – August 2015, Figure 24)
- Replacement of damaged filament cooling water tube in FPA cavity, again requiring cavity disassembly/reassembly (September 2015)

Testing of the power supply transformer and rectifiers after a blown fuse was discovered in a 13.8 kVAC fused disconnect switch (March-April 2016, Figure 25)

2.7 OTHER ACTIVITIES

Support was provided to move 28 GHz waveguide and components no longer needed by Mega-Amp Spherical Tokamak (MAST), and to maintain several gyrotrons (28, 35, and 53 GHz) and associated superconducting magnets.

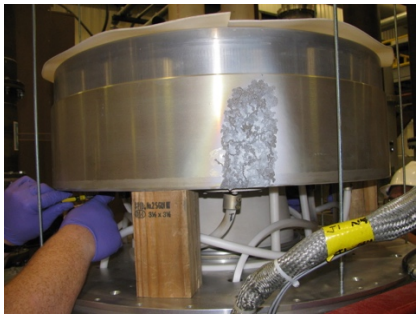

Fig. 24. Disassembly of damaged FMIT FPA cavity tuning structure.

Fig. 25. FMIT 13.8 kVA fused disconnect switch and vacuum contactors.

2.8 REFERENCES (CITED IN PROGRAM NARRATIVE)

1. C. Klepper et al., Phys. Rev. Lett. 110, 215005 (2013).
2. E.H. Martin et al., Plasma Phys. Control. Fusion 57, 065011 (2015).
3. E.H. Martin et al., AIP Conference Proceedings 1689, 030011 (2015).
4. H. Kohno and J.R. Myra, Comput. Phys. Commun. 220, 129 (2017).
5. E.H. Martin et al., Rev. Sci. Instrum. 87, 11E402, (2016).
6. A. Zafar et al, Rev. Sci. Instrum. 87, 11E505, (2016).
7. E.H. Martin, PhD thesis, North Carolina State University, (2014).
8. M. Madi et al, Plasma Phys. Control. Fusion 57, 125001 (2015).
9. J.L. Terry et al., J. Nucl. Mater. 390, 339 (2009).
10. C.C. Petty, et al., Nuclear Fusion 44, 243 (2004).
11. S. Coda, et al., Nuclear fusion, 43, 1361 (2003).
12. A.U. Team et al., Phys. Rev. Lett., 98, 025005 (2007).
13. T. Stange et al., EPJ Web of Conferences 157, 02008 (2017).
14. R. H. Goulding et al., Fusion Sci. Technol. 72, 588 (2017).
15. J.B.O. Caughman et al., J. Vac. Sci. Technol. A, 35, 03E114 (2017).
16. J. Rapp et al., IEEE Transactions on Plasma Science, 44, 3456 (2016).
17. P. Piotrowicz et al., “Direct measurement of the transition from edge to core power coupling in a light-ion helicon source”, Accepted for publication in Physics of Plasmas.
18. T. Biewer et al., Physics of Plasmas 25, 024501 (2018);
19. C.J. Beers et al., Physics of Plasmas, 25, 013526 (2018).

3. KEY PERSONNEL

Key research and engineering staff members for this program are listed in Table 3 and biographical information is provided following Table 3.

Table 3. Key personnel, job titles, and program roles

Name	Job Title	Program Role
John B. O. Caughman	Senior Research and Development (R&D) Staff	Diagnostics, RF power delivery and measurement
Richard H. Goulding	Senior R&D Staff	High power RF delivery including transmission line component development, tuning and matching development, and antenna design, modeling, and measurement
Elijah H. Martin	R&D Associate	Diagnostics development and application
Ian Campbell	Senior Technician	RF troubleshooting, diagnostics, electronics design/fabrication/testing
Jeff D. Bryan	Technical Staff Member	RF troubleshooting, diagnostics, transmitter maintenance, and testing
Gary L. Bell	Manager 3	Project Management
Name	**Job Title**	**Program Role**

John B. O. Caughman, Ph.D.
Senior R&D Staff
Fusion and Materials for Nuclear Systems Division
Nuclear Science and Engineering Directorate
Oak Ridge National Laboratory
Tel: 865-574-5131
caughmanjb@ornl.gov

Dr. Caughman is a senior staff scientist in the Fusion and Materials for Nuclear Systems Division of the Oak Ridge National Laboratory (ORNL), involved with radio frequency, microwave, and plasma technologies for magnetic fusion and non-fusion applications. He is the author or coauthor of over 60 papers published in journals and conference proceedings.

Since joining the research staff at ORNL in 1992, he has concentrated on research involving microwaves and high-power radio frequency (RF) antenna systems for fusion applications. He has extensive experience in modeling and testing antenna structures, measuring antenna fields and electrical parameters, and studying material erosion and deposition. Current fusion-related research includes microwave emission measurement diagnostics, high-voltage RF breakdown in antenna structures for magnetic fusion applications, microwave plasma production/heating, high-power microwave transmission line component development/testing, microwave cavity design for pellet (dielectric) mass detection, and design of components and experiments on EBW and whistler wave coupling to over-dense plasmas used in plasma material interaction research.

In the area of non-fusion related research, he has extensive experience related to the plasma processing of materials. Research experience includes development of large area plasma sources for material processing, RF system modeling, plasma diagnostics, plasma enhanced physical vapor deposition, and high-density plasma enhanced chemical vapor deposition of a variety of materials, including polycrystalline silicon, silicon nitride, tantalum oxide, copper, boron nitride, and carbon nanostuctures, as well as large-area non-contact power transfer techniques appropriate for transportation applications. He was recently the Co-Leader of the RF Diagnostics Task Force for SEMI (Semiconductor Equipment and Materials International) and was responsible for creating and writing Standards for the RF Equipment used in semiconductor manufacturing. In addition, he has designed, developed, and implemented systems for the RF heating of ceramics for armor applications and the heating of soils for detection of chemical contaminants.

Prior to joining ORNL, he worked at IBM from 1989 to 1992, where he conducted research to characterize the plasma physics of electron cyclotron resonant (ECR) plasma sources used in the manufacturing of semiconductor components. In 1991, he became co-leader of a group to develop and implement a plan for the use of real-time diagnostics to aid in the manufacturing of semiconductor devices and acted as a working interface between IBM Research and IBM Manufacturing.

Dr. Caughman received a Ph.D (1989) in Nuclear Engineering from the University of Illinois, where his thesis work was on the interaction between the plasma and the radio frequency (RF) fields on the surfaces of antennas. He received his M.S. degree in Nuclear Engineering from the University of Illinois in 1986 and his B.S. in Electrical Engineering from the University of South Carolina in 1984. From 2001-2004, he was the Chair of the Plasma Science and Technique Division of the International Union of Vacuum Science, Technique, and Applications (IUVSTA). In 2005, he was Chair of the Plasma Science and Technology Division of the American Vacuum Society (AVS) and teaches a 2-day short course on the Basics of RF Technology for the AVS. He is currently a member of the AVS, APS, and the IEEE.

Richard H. Goulding, Ph.D.

Senior R&D Staff

Fusion and Materials for Nuclear Systems Division
Nuclear Science and Engineering Directorate
Oak Ridge National Laboratory
Tel: 865-574-6480
gouldingrh@ornl.gov

Dr. Goulding is presently a Senior Research Staff Member in the Plasma Technology and Applications Group at Oak Ridge National Laboratory, and has more than thirty-five years of experience in the areas of the physics and technologies of ion cyclotron heating systems and RF-based plasma sources. He is the author or co-author of more than 80 papers published in journals and conference proceedings.

Since 2007 he has lead the R&D effort in the US ITER program to develop and test coaxial transmission line components, steady state matching systems, and control algorithms for the ITER Ion Cyclotron Heating and Current Drive system. Components developed as part of this work have demonstrated world leading steady-state power and voltage handling capability. Dr. Goulding also works with the ITER International Organization (IO) for the ITER Ion Cyclotron System to review designs of the antenna, transmission line and matching, and RF source systems.

He also led the effort to develop a light ion helicon plasma source that has operated successfully at power levels > 100 kW and is presently used in the Proto-MPEX (Prototype Material-Plasma Exposure eXperiment) linear plasma device. Proto-MPEX has produced world record plasma density for a helicon plasma source operating with deuterium. Dr. Goulding has also developed all aspects of the ion cyclotron heating system for Proto-MPEX.

Past activities include: Lead the development, design, fabrication, and testing of a High-Power Prototype of the Joint European Torus (JET) ITER-Like ICRF Antenna during 2001-2005, and participated in experiments on the final antenna at JET in 2008-2009, contributing to successful demonstration of coupling of ITER-relevant power densities to ELMy H-Mode plasmas.

Designed and operated Mini-RFTF/STX helicon source. Developed method for producing high density helicon plasmas using hydrogen gas. Designed, built, and operated helicon plasma source for VX1-VASIMR experiment at the Advanced Space Propulsion Laboratory at NASA Johnson Space Center.

Led program for Large Area Plasma Source Development – developed novel robust matching system, novel electronegative plasma stabilization technique, and improved RF coils for producing inductively coupled plasmas. Received an ORNL Technical achievement award for work in 1998.

Originated system using passive high power rf components to allow reliable ICRF operation in ELMing H-mode plasmas. The system presents a constant impedance to the final power amplifier in the presence of rapidly varying plasma loads. Designs based on this work are now in use on the JET and ASDEX-U tokamaks, and have been used on the DIII-D tokamak.

Designed, obtained funding for, and directed a series of novel experiments to measure RF parameters in dielectric materials in-situ during gamma and neutron irradiation in a TRIGA reactor.

Dr. Goulding did his thesis work developing a microwave startup system, and researched ion cyclotron plasma buildup in the Phaedrus-B Tandem mirror, as well as effects of RF and gas on plasma stability. He also designed, built, and operated plasma diagnostics: microwave interferometers, gridded energy analyzers, Langmuir probes, and soft x-ray detectors, and was a recipient of the David L. Gamage Memorial Fellowship.

Dr. Goulding received a Ph.D. in Nuclear Engineering and Engineering Physics (1987) from the University of Wisconsin, and M.S. (1982) and B.S. (1980) degrees in Nuclear Engineering, also from the University of Wisconsin. Dr. Goulding is a member of the American Physical Society.

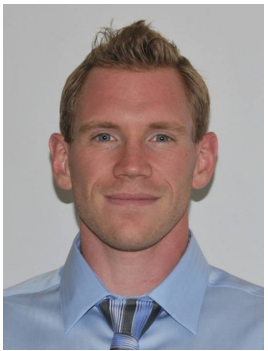

Elijah H. Martin, Ph.D.
Research and Development Associate
Nuclear Science and Engineering Directorate
Fusion and Materials for Nuclear Systems
Plasma Technology and Applications
martineh@ornl.gov

Elijah Martin has a background as an experimental plasma physicist (Ph.D., North Carolina State University 2014). Upon graduation, he accepted a postdoctoral fellowship administered by the US DOE Fusion Energy Postdoctoral Research Program. The fellowship was carried out in the Fusion and Materials for Nuclear Systems Division (FMNSD) at ORNL, where he developed a laser based spectroscopic diagnostic to measure plasma parameters and electric and magnetic fields. He is currently involved with a multi-institutional (Plasma Science and Fusion Center at MIT, DIII-D at General Atomics, WEST at IRFM in France, and LLNL) synergistic experimental/simulation effort to understand the interaction of the plasma edge with wave fields generated by heating and current drive systems of magnetic confinement fusion devices. He is leading the experimental effort by providing a spectroscopic diagnostic capable of measuring wave fields non-perturbatively using passive polarized optical emission spectroscopy. His research conducted at ORNL is focused on further development of laser-based spectroscopy and involves the mentoring of a doctoral graduate student. His research has shown that the resolution of measurable parameters can be increased by nearly two orders of magnitude when compared to passive polarized optical emission spectroscopy. The purpose of this work is to provide an unprecedented direct path for model validation via experiments.

Gary L. Bell, Ph.D.

Plasma Materials & Application Group, Group Leader
Fusion and Materials for Nuclear Systems Division
Nuclear Science and Engineering Directorate
Oak Ridge National Laboratory

Dr. Gary Bell became the Plasma Technology and Applications Group Leader in April 2013. The group is focused on the development of plasma heating and fueling technologies and the development of capabilities to support the growing area of plasma-materials interaction science.

Gary joined ORNL in 1992 in the Metals and Ceramics Division (M&C) where he worked on the design and analysis of irradiation experiments on highly enriched uranium coated-particle fuels for High Temperature Gas-Cooled Reactors. He then transferred to the Fusion Energy Divisionwhere for 10 years his work included experimental measurements and antenna modeling to advance the application of high power RF heating in magnetic confinement fusion experiments and RF measurement and power delivery system characterization supporting U.S. semiconductor manufacturing. During this time he served as the Plasma Diagnostics Group Leader at SEMATECH in Austin, TX (two-year off-site assignment).

From 2003-2007 Gary served as the national co-lead for the DOE-NE Advanced Gas Reactor Fuel Development and Qualification (AGR) Program, leading a multi-directorate ORNL team to develop coated particle fuel for high temperature reactor applications and fabricating fuel that set a new global record for in-core performance. Gary led the ORNL portion of the team that won the 2010 inaugural Gordon Battelle Prize for Technology Impacts – *Next Generation Fuel for High Temperature Gas-Cooled Reactors*, comprising researchers from ORNL, INL, Babcock & Wilcox, and General Atomics.

Gary established the Nuclear Fuel and Materials (NFM) Group in the Materials Science and Technology Division in 2005 and served as its group leader until April 2013, with the exception of a two-year hiatus to work in the Coupled End-to-End Demonstration Project, an integrated test bed for the research, development, and demonstration of nuclear fuel cycle separation and conversion technologies tasked with identifying and resolving interfacial issues between the various steps in the processing of used nuclear fuel. He led the R&D team that fabricated proof of principle U-Pu-Np oxide fuel pellets using material recycled - without isolating the plutonium - from fuel used at the Dresden Nuclear Power Plant. In his role as the NFM Group Leader, he provided leadership for a variety of nuclear fuel cycle technical and infrastructure projects supporting nuclear fuel and target development, including transmutation fuel feedstock R&D, radioisotope R&D and production, Tristructural-isotropic coated particle fuel for Light Water Reactor applications, and irradiation testing of advanced fuel materials.

Gary earned a Doctorate degree in Plasma Physics from Auburn University in 1990. He performed his thesis work (electron cyclotron emission and absorption) at ORNL on the Advanced Toroidal Facility (stellarator) and worked as a post-doctoral researcher on coated particle fuel irradiation testing in ORNL's M&C Division 1990-1992.

4. PRODUCTS

The products of the program include conference papers and presentations, journal articles, equipment maintenance, repairs and upgrades. Written products that were supported by or used the major equipment supported by this program are listed below. These include a set of export-controlled test reports and design calculations produced for US ITER and circulated to the ITER International Organization that are not publicly available.

4.1 JOURNAL ARTICLES

1. J. Rapp, T. M. Biewer, T. S. Bigelow, J. F. Caneses, J. B. O. Caughman, S. J. Diem, R. H. Goulding, R. C. Isler, A. Lumsdaine, C. J. Beers, T. Bjornholm, C. Bradley, J. M. Canik, D. Donovan, R. C. Duckworth, R. J. Ellis, V. Graves, D. Giuliano, D. L. Green, D. L. Hillis, R. H. Howard, N. Kafle, Y. Katoh, A. Lasa, T. Lessard, E. H. Martin, S. J. Meitner, G. N. Luo, W. D. McGinnis, L. W. Owen, H. B. Ray, G. C. Shaw, M. Showers, V. Varma, and the MPEX Team, "Developing the science and technology for the Material Plasma Exposure eXperiment", Nuclear Fusion **57,** 11601 (2017).
2. N. Kafle, Larry Owen, J. F. Caneses, T. M. Biewer, D. Donovan, J. Rapp, M. A. Showers, J. B. O. Caughman and R. H. Goulding, "Plasma transport on Prototype-Material Plasma Exposure eXperiment (Proto-MPEX) and comparison with B2-Eirene modelling in high density discharges," submitted for publication to Physics of Plasmas.
3. M. A. Showers, P. A. Piotrowicz, C. J. Beers, T. M. Biewer, J. F. Caneses, J. B. O. Caughman, D. Donovan, R. H. Goulding, A. Lumsdaine, N. Kafle, L. W. Owen, J. Rapp, H. B. Ray, "Power accounting in the helicon region of plasma discharges in the linear device Proto-MPEX", Plasma Physics and Controlled Fusion **60**, 065001 (2018).
4. C. Thomas, T. M. Biewer, L. R. Baylor, S. K. Combs, S. J. Meitner, J. Rapp, D. L. Hillis, E. Granstedt, R. Majeski and R. Kaita, "Design of a digital holography system for PFC erosion measurements on Proto-MPEX," Review of Scientific Instruments, **87,** 11D624 (2016).
5. M. A. Showers, T. M. Biewer, J. B. O. Caughman, D. Donovan, R. H. Goulding, J. Rapp, Heat flux estimates of power balance on Proto-MPEX with IR imaging," Review of Scientific Instruments, **87**, 11D412 (2016).
6. J. F. Caneses, B. D. Blackwell, and P. Piotrowicz, "Helicon antenna radiation patterns in a high-density hydrogen linear plasma device," Physics of Plasmas **24**, 113513 (2017).
7. R. H. Goulding, J. B. O. Caughman, J. Rapp, T. M. Biewer, T. S. Bigelow, I. H. Campbell, J. F. Caneses, D. Donovan, N. Kafle, E. H. Martin, H. B. Ray, G. C. Shaw, M. A. Showers, "Progress in the Development of a High Power Helicon Plasma Source for the Materials Plasma Exposure Experiment," Fusion Science and Technology **72** 588 (2017).
8. J. B. O. Caughman, R. H. Goulding, T. M. Biewer, T. S. Bigelow, I. H. Campbell, J. Caneses, S. J. Diem, A. Fadnek, D. T. Fehling, R. C. Isler, E. H. Martin, C. M. Parish, J. Rapp, K.Wang, C. J. Beers, D. Donovan, N. Kafle, H. B. Ray, G. C. Shaw, and M. A. Showers, "Plasma source development for fusion-relevant material testing", Journal of Vacuum Science and Technology A, **35**, 03E114 (2017).
9. C. J. Beers, R. H. Goulding, R. C. Isler, E. H. Martin, T. M. Biewer, J. F. Caneses, J. B. O. Caughman, N. Kafle and J. Rapp, "Helicon Plasma Ion Temperature Measurements and Observed Ion Cyclotron Heating in Proto-MPEX," Physics of Plasmas, **25**, 013526 (2018).
10. M. A. Showers, T. M. Biewer, J. B. O. Caughman, D. Donovan, R. H. Goulding, Arnold Lumsdaine and J. Rapp "Helicon Power Source Analysis of the Prototype Material Exposure

eXperiment (Proto-MPEX) using Fluoroptic Probes,", submitted for publication to Plasma Sources Science and Technology.

11. T. Biewer and G. Shaw, “Initial implementation of a Thomson scattering diagnostic for Proto-MPEX,” Review of Scientific Instruments, **85**, 11D812 (2014).
12. T. M. Biewer, T. S. Bigelow, J. F. Caneses, S. J. Diem, D. L. Green, N. Kafle, J. Rapp "Observations of electron heating during 28 GHz microwave power application in Proto-MPEX," Physics of Plasmas, **25**, 024501 2018.
13. J. Rapp, J. M. Canik, J. D. Lore, J. F. Caneses, N. Kafle, H. B. Ray and M. A. Showers, “Radial Transport Modeling of High Density Deuterium Plasmas in Proto-MPEX with the B2.5-EIRENE Code,” Plasma Physics and Controlled Fusion.
14. L. W. Owen, J. Rapp, J. M. Canik, Jeremy Lore, "Transport modeling of convection dominated helicon discharges in Proto-MPEX with the B2.5-Eirene code," Physics of Plasmas, **24**, 112504 (2017).
15. J. Rapp, L. W. Owen, X. Bonnin, J. F. Caneses, J. M. Canik, C. Corr, J. D. Lore, ‘Transport similations of linear plasma generators with the B2.5-Eirene and EMC3-Eirene codes”, Journal of Nuclear Materials, **463**, 510 (2015).
16. E.H. Martin M. Goniche, C. C. Klepper, J. Hillairet, R. C. Isler, C. Bottereau, L. Colas, A. Ekedahl, S. Panayotis, B. Pegourie, P. Lotte, G. Colledani, J. B. Caughman, J. H. Harris, D. L. Hillis, S. C. Shannon, F. Clairet, X. Litaudon, “Electric field determination in the plasma-antenna boundary of a lower-hybrid wave launcher in Tore Supra through dynamic Stark-effect spectroscopy, Plasma Physics and Controlled Fusion **57**, 065011 (2015).
17. E. H. Martin, A. Zafar, J. B. O. Caughman, R. C. Isler, G. L. Bell,” Applications of Doppler-free saturation spectroscopy for edge physics studies,”, Review of Scientific Instruments **87**, 11E402 (2016).
18. A. Zafar, E. H. Martin, S. C. Shannon, R. C. Isler, and J. B. O. Caughman, “A temporally and spatially resolved electron density diagnostic method for the edge plasma based on Stark broadening,” Review of Scientific Instruments **76** 11E505 (2016).

4.2 ABSTRACTS/PRESENTATIONS

1. T. S. Bigelow, J. B. O. Caughman, C. Dukes, R.H. Goulding, J. Rapp, S. Diem and T.Biewer ,"A 28 GHz 200 kW generation and launching system for ECH/EBW on Proto-MPEX at ORNL," 2014 International Conference on Plasma Science, May 27-30, 2014, Washington, VA.
2. C. J. Beers, G. Shaw, T. M. Biewer, J Rapp, "Characterization of ion fluxes and heat fluxes for PMI relevant conditions on Proto-MPEX," American Physical Society-Division of Plasma Physics, October 31-November 4, 2016, San Jose, CA, 2016.
3. C. Morean, T. M. Biewer, G. Shaw, C. J. Beers and H. B. Ray, "Spatial and Temporal characterization of plasma properties via emission spectroscopy in fusion materials testing device Proto-MPEX," American Physical Society-Division of Plasma Physics, October 31-November 4, 2016, San Jose, CA, 2016.
4. "The diagnosing of plasmas using spectroscopy and imaging on Proto-MPEX," T. M. Biewer, K-Cie Baldwin, Jackson Crouse Powers, Randi Hardin, Sylas Johnson, Ava McCleese, G. Shaw, M. A. Showers and Christian Skeen, American Physical Society Division of Plasma Physics Conference, Savannah, GA, November 16-20, 2015.
5. R. H. Goulding, M. P. McCarthy, C. E. Deibele, D. A. Rasmussen, D. W. Swain, G.C C. Barber, I. H. Campbell, S. L. Gray, R. L. Moon, P. V. Pesavento, R. M. Sanabria, E. Fredd, N. Greenough, C. Kung, “Component tests for the ITER Ion Cyclotron Transmission Line and

Matching System – Status and Plans", American Physical Society Division of Plasma Physics Conference, Savannah, Georgia, November 16-20, 2015.

6. R. H. Goulding, J. B. O. Caughman, J. Rapp, T. M. Biewer, I. H. Campbell, J. F. Caneses, N. Kafle, H. B. Ray, M. A. Showers, P. A. Piotrowicz, "Ion Cyclotron Heating on Proto-MPEX," American Physical Society Division of Plasma Physics Conference, San Jose, California, October 31-November 4, 2016, San Jose, CA, 2016.
7. H. B. Ray, T. M. Biewer, J. Green, E. G. Lindquist, L. McQuown and O. Schmitz, "Development and Implementation of a New HELIOS Diagnostic using a Fast Piezoelectric Valve on Proto-MPEX," American Physical Society - Division of Plasma Physics Conference, October 23-27, Milwaukee, WI, 2017.
8. R. Dhaliwal, T. M. Biewer, R. C. Isler, C. C. Klepper, E. H. Martin and J. Rapp, "Doppler spectroscopy on plasma discharges produced in Proto-MPEX," American Physical Society Division of Plasma Physics Conference, Savannah, Georgia, November 16-20, 2015.
9. T. S. Bigelow, J. F. Caneses, J. B. O. Caughman, S Diem, David Green, R. W. Harvey, Yu. Petrov and J. Rapp,"EBW propagation and damping in Proto-MPEX," American Physical Society (APS-DPP, San Jose, CA, 2016).
10. T. S. Bigelow, J. B. O. Caughman, S. J. Diem, R. H. Goulding, T. M. Biewer and J. Rapp, "ECH/EBW Heating of Proto-MPEX Plasmas," 43rd IEEE International Conference on Plasma Science, June 19-23, 2016, Banff, Canada.
11. M. A. Showers, T. M. Biewer, T. S. Bigelow, J. B. O. Caughman, D. Donovan, R. H. Goulding, T. Gray, J. Rapp, D. Youchison and R. Nygren, "Estimates of heat flux to material surfaces in Proto-MPEX with IR imaging," American Physical Society Division of Plasma Physics Conference, Savannah, GA, 2015.
12. T. M. Biewer, Steven Meitner, J. Rapp, H. B. Ray and G. Shaw, "First results from the Thomson scattering diagnostic on Proto-MPEX," 21st Topical Conference on High- Temperature Plasma Diagnostics, June 5-9, 2016. Madison, WI.
13. C. J. Beers, T. M. Biewer, J. F. Caneses, J. B. O. Caughman, S. J. Diem, R. H. Goulding, D. L. Green, N. Kafle, J. Rapp and T. S. Bigelow, "High power plasma heating experiments on the Proto-MPEX facility," 59th Annual Meeting of the APS Division of Plasma Physics, October 23-27, Milwaukee, WI, 2017.
14. R. H. Goulding, M. P. McCarthy, C. E. Deibele, D. A. Rasmussen, D. W. Swain, G. C. Barber, G. L. Bell, C. N. Barbier, I. H. Campbell, E. Fredd, N. Greenough, C. Kung, R. L. Moon, P. V. Pesavento, "Results of Transmission Line Component Testing for the ITER Ion Cyclotron Heating and Current Drive System", 21st Topical Conference on RF Power in Plasmas, Lake Arrowhead, CA, 2015.
15. J. B. O. Caughman, R. H. Goulding, T. M. Biewer, T. S. Bigelow, I. H. Campbell, S. J. Diem, E. H. Martin, P. Pesevento, J. Rapp, H. B. Ray and G. Shaw, "Initial Operation of the Proto-MPEX High Intensity Plasma Source," 21st Topical Conference on RF Power in Plasmas, Lake Arrowhead, CA, 2015.
16. R. H. Goulding, C. E. Deibele, D. A. Rasmussen, G. C. Barber, I. H. Campbell, M. P. McCarthy, and D. W. Swain, "Developments in the Testing of ITER Ion Cyclotron Transmission Line Components," 22nd Topical Conference on RF Power in Plasmas, Aix-en-Provence, France, 2017.
17. P. A. Piotrowicz, D. Ruzic, J. F. Caneses, J. B. O. Caughman, R. H. Goulding, David Green, Jeremy Lore and J. Rapp, "Ion Cyclotron Resonance Heating on Proto-MPEX," The 45th IEEE International Conference on Plasma Science, Denver, CO.
18. J. B. O. Caughman, R. H. Goulding, Clyde Beers, T. M. Biewer, T. S. Bigelow, J. F. Caneses, S. J. Diem, David Green, N. Kafle, Ralph Isler, P. A. Piotrowicz, J. Rapp and M. A. Showers,

"Measurements of ion energies during plasma heating of the Proto-MPEX High Intensity Plasma Source," 59th Annual Meeting of the APS Division of Plasma Physics, October 23-27, Milwaukee, WI, 2017.

19. T. M. Biewer, K. Collins, B. Johnson, A. Lancaster, R. Mosby, H. B. Ray, G. Shaw and B. Young, "Measurements of the relative transmission properties of optical fiber for use on Proto-MPEX," American Physical Society Division of Plasma Physics Conference, New Orleans, LA, 2014.
20. C. Skeen, T. M. Biewer, C. Cantrell, J. Klemm, R. Musick, G. Nunley, J. S. Sanchez, D. Sawyer, H. B. Ray, G. Shaw and M. A. Showers, "Measuring the parameters of a high flux plasma in Proto-MPEX," American Physical Society Division of Plasma Physics Conference, San Jose, CA, 2016.
21. P. A. Piotrowicz, J. F. Caneses, R. H. Goulding, David Green, J. B. O. Caughman and David Ruzic, "Modeling and Theory of RF Antenna Systems on Proto-MPEX," 59th Annual Meeting of the APS Division of Plasma Physics, October 23-27, Milwaukee, WI, 2017.
22. T. M. Biewer, T. S. Bigelow, J. F. Caneses, J. B. O. Caughman, R. Dhaliwal, D. Donovan, D.Fehling, R. H. Goulding, N. Kafle, D. L. Hillis, E. H. Martin, S. J. Meitner, R. Mosby, J. Rapp, H. B. Ray, G. Shaw and M. A. Showers, "Overview of diagnostic implementation on Proto-MPEX at ORNL," International Workshop on Plasma Materials Interaction Facilities for Fusion Research, Juelich, Germany, 2015.
23. M. A. Showers, T. M. Biewer, J. B. O. Caughman, D. Donovan, R. H. Goulding and J. Rapp, "Particle and heat flux estimates in Proto-MPEX in Helicon Mode with IR imaging," 58th Annual Meeting of the APS Division of Plasma Physics, San Jose, CA, 2016.
24. "Plasma Heating in the Proto-MPEX Plasma Device," J. B. O. Caughman, T. M. Biewer, T. S. Bigelow, Clyde Beers, J. F. Caneses, S. J. Diem, David Green, R. H. Goulding, N. Kafle, Ralph Isler, P. A. Piotrowicz, J. Rapp and M. A. Showers, 6th International Workshop on Plasma Material Interaction Facilities for Fusion Research (PMIF2017), Tsukuba, Japan, 2017.
25. G. Shaw, M. Martin and T. M. Biewer, "Preliminary Design of Laser-induced Breakdown Spectroscopy for proto-MPEX," 20th Topical Conference on High-Temperature Plasma Diagnostics (HTPD 2014), Atlanta, GA, 2014.
26. M. A. Showers, Clyde Beers, T. M. Biewer, J. F. Caneses, J. B. O. Caughman, D. Donovan, A. Lumsdaine, N. Kafle, L. W. Owen, H. B. Ray, J. Rapp and D. Youchison, "Preliminary Energy Balance Analysis of Proto-MPEX," 59th Annual Meeting of the APS Division of Plasma Physics, Milwaukee, WI, 2017.
27. E. H. Martin, D. Donovan, APS Division of Plasma Physics, "Utilization of Double Langmuir Probes on Proto-MPEX," N. Kafle, J. B. O. Caughman, J. F. Caneses, R. H. Goulding, 58th Annual Meeting of The APS Division of Plasma Physics, October 31-November 4, 2016. San Jose, CA, 2016.
28. A. Zafar, E. H. Martin, S. Shannon, "A Plasma Edge Electron Density Diagnostic Based on a Doppler-Free Measurement of Stark Broadening", 59th Annual Meeting of the APS Division of Plasma Physics, October 23-27, Milwaukee, WI.
29. E. H. Martin, "Lower Hybrid Wave Electric Field Vector Measurements Using Non-Perturbative Dynamic Stark Effect Optical Spectroscopy on Alcator C- Mod, 59th Annual Meeting of the APS Division of Plasma Physics, October 23-27, Milwaukee, WI.

4.3 PROCEEDINGS

20. R. C. Duckworth, J. A. Demko, A. Lumsdaine, J. Rapp, T. Bjorholm, R. H. Goulding, J. B. O. Caughman, W. D. McGinnis, "Cryogenic Considerations for Superconducting Magnet Design for the Material Plasma Exposure eXperiment (MPEX)," Presented at the 2015 Cryogenic Engineering Conference (CEC)2015, Tucson, AZ, June 28-July2 2015, IOP Conference Series: Materials Science and Engineering, **101** 012143 (2015).
21. J. Rapp , T. M. Biewer , T. Bigelow , J. B. O. Caughman , R. Duckworth , D. Giuliano , R. H. Goulding , D. L. Hillis , R. Howard , R. J. Ellis , T. Lessard , J. D. Lore , A. Lumsdaine , E. Martin , W. D. McGinnis , S. J. Meitner, et al., "The Material Plasma Exposure eXperiment MPEX: Pre-design, development and testing of source concept," Presented at the 20th IEEE Pulsed Power Conference/26th Symposium on Fusion Engineering (PPC/SOFE) 2015, Austin, TX, May 31-June 4 2015, 2015 IEEE 26th Symposium on Fusion Engineering (SOFE), pp. 1-8.

4.4 OTHER (US ITER REPORTS)

1. R. H. Goulding, "Procedure for Performing High-Power Tests on ICH Transmission Line Components Using a Resonant Ring - EXPORT CONTROL," US_D_236DNQ, ITER_D_UXFWLU.
2. R. H. Goulding, M. P. McCarthy, "Test Plan for the ICH Pressurized Blower," US_D_23GDHC, ITER_D_URQG4X.
3. R. H. Goulding, M. P. McCarthy, I. H. Campbell, "Preliminary Test Report on the ICH Pressurized Blower Test Article," US_D_22WV84, ITER_D_URCJR5.
4. R. H. Goulding, I. H. Campbell, P. V. Pesavento, "Test Report on First-Generation ICH 50 Ohm Gas Barriers - EXPORT CONTROL," US_D_23AGPY, ITER_D_UPU7PB.
5. R. H. Goulding, I. H. Campbell, M. P. McCarthy, P. V. Pesavento, "Test Report on ICH Center Conductor Supports for Spoke Ring Assembly (SRA) Straights and Elbows - EXPORT CONTROL," US_D_23LAR7, ITER_D_UPUUXL.
6. R. H. Goulding, M. P. McCarthy, I. H. Campbell, P. V. Pesavento, "Test Report on an Ion Cyclotron Heating (ICH) Assembly Bellows Test Article - EXPORT CONTROL," US_D_2369WT, ITER_D_UPT9EB.
7. R. H. Goulding, "Test Plan for ICH 50 Ohm Characteristic Impedance Test Articles - EXPORT CONTROL," US_D_239CPC, ITER_D_RZDV26.
8. R. H. Goulding, "Procedure for Performing High Voltage and High Current Tests on Ion Cyclotron Transmission Line Components Using a Resonant Line - EXPORT CONTROL," US_D_23EM3M, ITER_D_TRC8BU.

5. FACILITIES, EQUIPMENT, AND OTHER RESOURCES

The RF Technology program uses the Plasma Applications Laboratory located at ORNL in Bldg. 5800, Rm C101, the Multi-program High Bay Facility, and Bldg. 7604 (for equipment storage). The space charge and utilities are paid from the Fusion and Materials for Nuclear System Division's organization burden account, costing $92,635 for C101, $584,417 for program specific portions of Bldg. 7625, $45,614 for Bldg. 7627, and $8,065 for Bldg. 7604 in FY2017. In addition, four SeaLand containers (no annual cost) are used for storage of equipment utilized by the program in years past. The program has benefitted during this reporting period from laboratory investments in scroll pumps to replace aging oil roughing pumps, software license renewals, oscilloscopes, electrical safety equipment, test and measurement equipment, optical components, data acquisition equipment, equipment storage cabinets, and lab benches, as well as repairs to test and measurement equipment, totaling $202,956 in FY2014, $88,665 in FY2015, $175,631 in FY2016, and 183,527 in FY2017 (4 year total = $650,779).

Experiments are performed primarily at the Multi-Program High Bay Facility (Building 7625, Figure 26) and the Room C-101 laboratory in Building 5800. Building 7625, together with the neighboring building 7627 housing magnet power supplies and the Thales transmitter, contain extensive infrastructure supporting the work described here including

- Two 5 MW DC power supplies currently used for Proto-MPEX magnets supplying 9000 A pulsed, 7500 A steady state, at 650 V (Figure 27)
- Two 500 kW DC power supplies, also used for Proto-MPEX magnets, supplying 5000 A steady state at 100 V
- Several high-power microwave sources including a 28 GHz, 200 kW gyrotron and a 140 GHz, 400 kW gyrotron. These are presently being or will be used for electron heating on Proto-MPEX via EBW, ECH, and collisional damping.
- Several high-power RF sources including:
    - A Continental FMIT transmitter with 40-80 MHz frequency range, operating at up to 1 MW for 30 s pulses, 500 kW steady state, as well as two 1 MW steady state dummy loads. This equipment is used for all high-power testing of ITER ion-cyclotron components (Figure 28)
    - A Continental FRT-86 transmitter with a frequency range 3-30 MHz supplying ~ 130 kW for 0.5 s pulses, 100 kW steady state, used to power the Proto-MPEX helicon plasma source. It can also be used for ICH on Proto-MPEX
    - A Continental FRT-85 transmitter with a frequency range 3-30 MHz supplying 30 kW for 0.5 s pulses, 20 kW steady state, used for ICH on Proto-MPEX
    - A Sairem 13.56 MHz fixed frequency RF generator, 100 kW steady state, used to power the Proto-MPEX helicon plasma source (Figure 29). Also, a combiner network has been constructed to combine its output with that of the FRT-86 (Figure 30).
    - A Thales 3-26 MHz transmitter supplying up to 1 MW steady state. The transmitter is not yet operational but will be used to supply up to 400 kW of ICH for Proto-MPEX and MPEX as funding permits.
- A deionized water system that includes two cooling towers with a maximum total continuous heat rejection capability of 8 MW. The system was upgraded in FY2016-17 using ORNL provided funds ($250k investment), with the chief improvement being the replacement of a damaged cooling tower by a new one (Figure 31). This has provided for the first time the ability to run multiple large experiments simultaneously in the building and makes the cooling system consistent with a 50% increase in electrical power for the building that was installed over the previous two years ($175k Facilities and Operations investment).
- The Proto-MPEX device itself (Figure 32), a linear device approximately 5 m in length utilizing 12 magnet coils from the Elmo Bumpy Torus (several spare coils also available) operating at up

to 9 kA and producing ≥ 1.5 T in the magnet bore, together with an extensive vacuum system that includes three 660 cfm Leybold Roots blowers and several Pfeiffer and Balzers turbo-pumps with nominal pumping speeds up to 2500 l/s. The device has an extensive suite of diagnostics including Thomson scattering at multiple axial and radial locations, passive spectroscopy using a McPherson spectrometer, a HoloSpec survey spectrometer, and filterscopes, fast visible light and Infrared (IR) cameras, soft x-ray detectors, retarding field energy analyzers, Langmuir probes, and others.

- RF high power test fixtures including a 6 MW resonant ring (Figure 33) and 100 kV resonant line (Figure 34), supporting the ITER ICH component testing.
- Both Proto-MPEX and ITER ICH tests utilize extensive PXI-based data acquisition and control systems using primarily National Instruments CPUs, IO modules, and fast A/Ds.

In addition, the laboratory in Building 5800 Room C-101 was upgraded in order to carry out the research on Doppler-free saturation spectroscopy. A significant amount (~$50k) of support systems were added during this upgrade. This included the installation of six 3-phase 208V 20A circuits, chilled water and compressed air lines/manifolds, cable tray, 3-channel gas delivery system, and a high-speed data acquisition system. Figure 35 depicts an image of the various support systems installed during the experimental test-stand upgrade.

We have included fact sheets that give further information about both the Building 7625 and Laboratory C-101 facilities. These are presented here as Figures 36 and 37.

Fig. 26. Exterior and interior views of Building 7625 Multi-Purpose High Bay Facility.

Fig. 27. 5 MW Magnet DC Power Supplies.

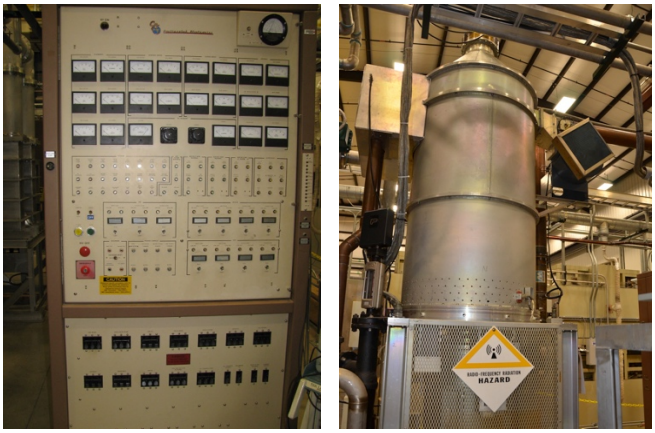

Fig. 28. FMIT transmitter control unit (left) and final power amplifier tetrode output cavity (right).

Fig. 29. Sairem 13.56 MHz 100 kW RF Generator.

Fig. 30. A portion of the 200 kW combiner network to be used with the Proto-MPEX helicon plasma source.

Fig. 31. View of south side of Building 7625 showing new cooling tower. The remaining original cooling tower is located to its left.

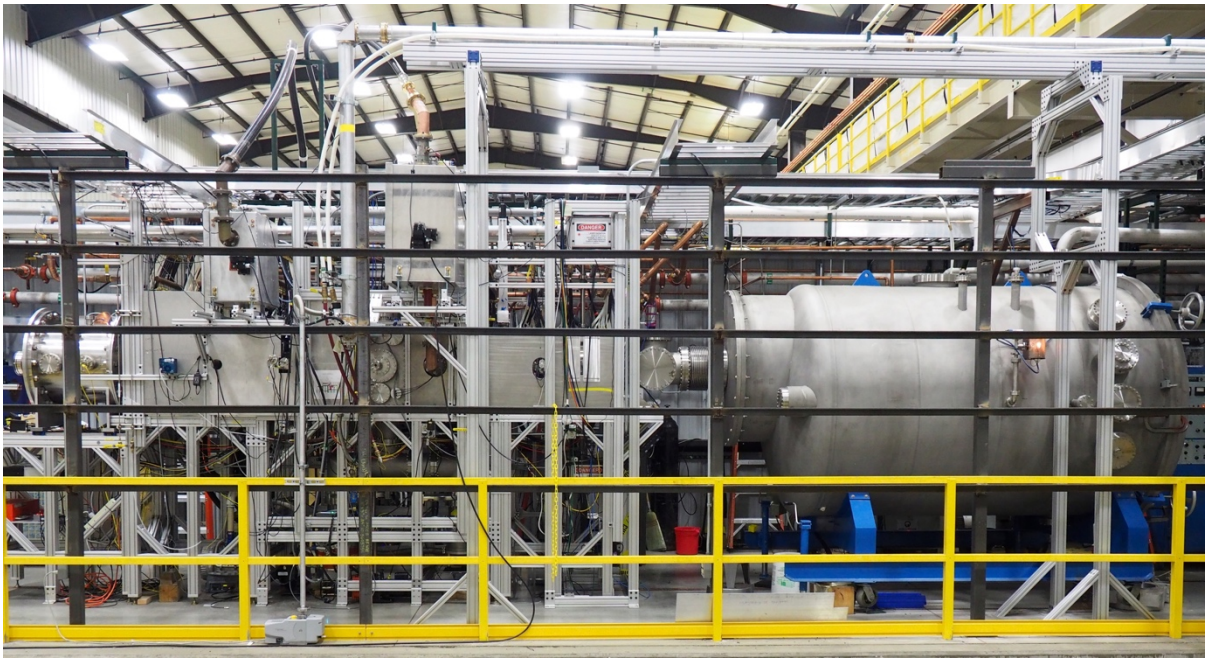

Fig. 32. Proto-MPEX linear plasma-materials interaction device.

Fig. 33. 6 MW resonant ring RF test fixture.

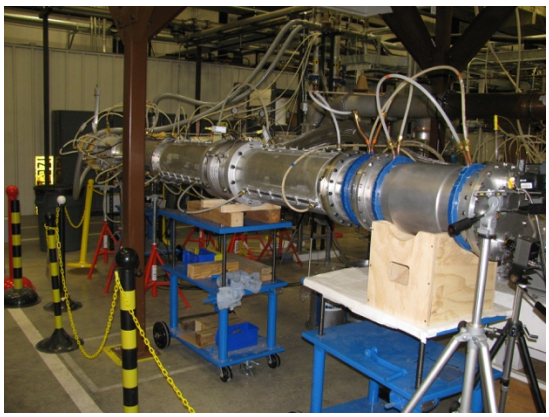

Fig. 34. 100 kV resonant line test fixture.

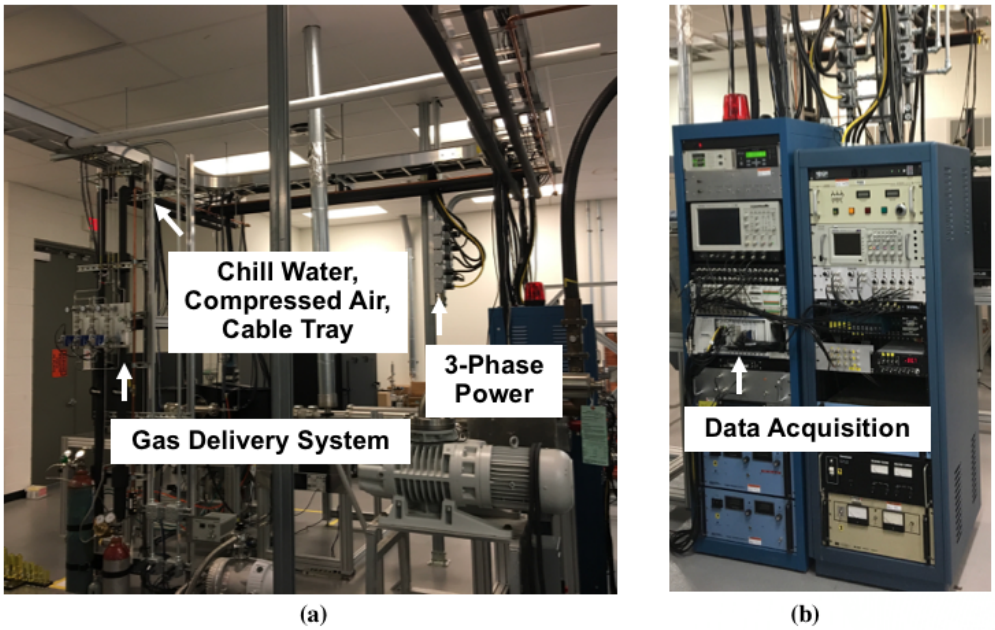

Fig. 35. (a) Image of the upgraded experimental test-stand highlighting the added support systems: 3-phase power, chill water, compressed air, cable tray. (b) Image of hardware used to power, control, and acquire data from the experimental test stand.

Multi-Program High Bay Facility (Buildings 7625/7627)

Installing a 4 mm microwave interferometer on Proto-MPEX to measure plasma density

7625 high bay supports Proto-MPEX helicon plasma source and plasma materials interaction R&D

Description

The Multi-Program High Bay Facility comprises buildings 7625 and 7627 and provides space and infrastructure for multiple research & development programs and projects primarily through ORNL's Fusion and Materials for Nuclear Systems Division. Sixteen individual lab spaces with a combined total gross floor area of over 33,000 square feet typically support 10-15 scientists, technicians, and other operations personnel depending on research experiment status.

In Building 7625, a variety of experimental projects are in progress, and currently include

- High power radiofrequency (RF) transmission line component testing for ITER;
- Plasma material interaction experiments and plasma source development using the Prototype Materials Plasma Exposure eXperiment (Proto-MPEX);
- Microwave-assisted plasma processing of materials;
- High temperature superconductivity component and device testing;
- High power electron cyclotron transmission line testing for ITER;
- Electrothermal plasma source development; and
- Specialized helium and hydrogenic species pump testing for ITER.

A set of RF generators (from 3 to 80 MHz ranging from 20 kW to 500 kW steady state and up to 1.5 MW pulsed) and microwave sources (from 18 to 140 GHz at 8 to 400 kW steady state) support experimental operations. A microwave development laboratory, an electronics lab, a laser diagnostics lab, an electrical distribution room, and a small machine shop area provide experiment support. Experiment cooling is provided by a demineralized water system with a cooling tower capable of dissipating 4 MW steady state.

Building 7627 houses high voltage power supply systems supporting experimental operations in Building 7625. These include a pair of 90 kV gyrotron supplies (900 kW and 1.4 MW steady state), high current magnet power supplies, and a tunable 3-27 MHz, 1 MW, steady state RF transmitter. The incoming power capacity is 48 MW, sufficient to power the current experimental demand with headroom for future experimental programs.

Contact

Michael A. Harper
Facility Manager
Oak Ridge National Laboratory
865.574.7299
harperma@ornl.gov

ornl.gov

ORNL is managed by UT-Battelle for the US Department of Energy

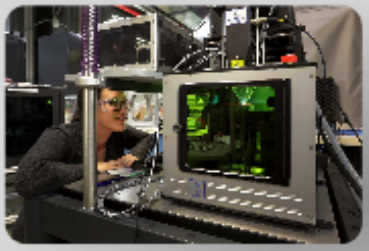

A University of Tennessee Knoxville graduate student uses Laser Induced Break-down Spectroscopy in the Laser Diagnostics Lab to characterize the effects of exposing materials to plasmas

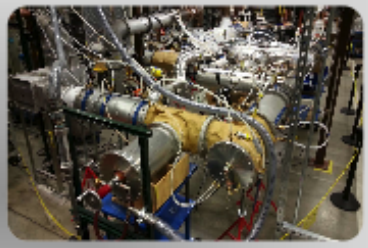

The Radio Frequency Test Facility for Transmission Lines is used to provide high voltage and high current conditions for testing RF transmission line components consistent with 6 MW steady state operation for up to 1 hour

Date: April 2017

OAK RIDGE National Laboratory

U.S. DEPARTMENT OF ENERGY

Fig. 36. Fact sheet for Building 7625 Mult-Program High Bay Facility.

Plasma Applications Laboratory

Description

The Plasma Applications Laboratory is a multi-functional laboratory that is used for experiments involving plasmas and radio frequency (RF) technology. The work focuses on technology development for both magnetic fusion research and non-fusion research applications. Various vacuum and plasma chambers are used for plasma source development, material deposition, plasma diagnostic development, RF sheath physics, and fundamental physics studies of RF breakdown phenomena in magnetic field and plasma environments. RF power supplies, ranging from 10 kHz to 28 GHz with power levels to 20 kW, are used for making plasmas and testing hardware. Network analyzers in the range from 1 kHz to 20 GHz are used to characterize RF and microwave components used in a wide variety applications.

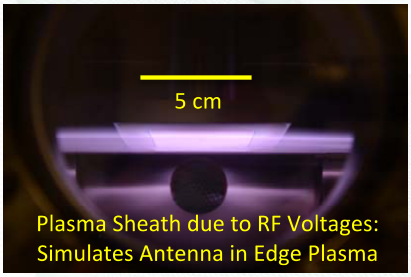

Plasma Sheath due to RF Voltages: Simulates Antenna in Edge Plasma

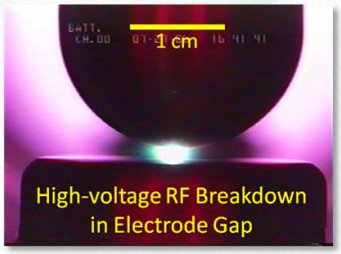

High-voltage RF Breakdown in Electrode Gap

Applications

- High-voltage RF breakdown for fusion antenna applications
- Advanced laser-based spectroscopy development for RF electric field measurements
- Advanced optical diagnostic development for plasma characterization
- RF sheath physics and near-field antenna interactions
- Plasma source development for materials processing and isotope production
- Plasma enhanced chemical vapor deposition
- Antenna 3-D field measurement system for launcher development
- High-power wireless power transfer
- High-power RF calibration of sensors for industry
- RF system characterization for semiconductor processing
- Electric field breakdown in liquids
- Microwave radiometer calibration and development
- Microwave cavity development for cryogenic pellet mass determination
- Network/impedance analysis of RF and microwave components
- Vacuum component development and leak-checking
- Custom electronics prototype development

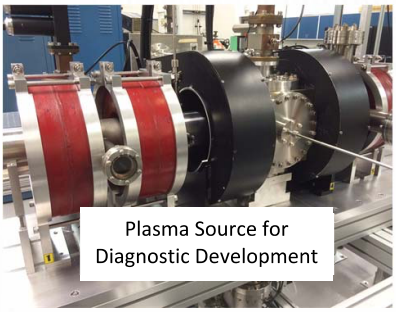
Plasma Source for Diagnostic Development

Date: April 2017

Contact

John Caughman
Senior Research Staff Member
Oak Ridge National Laboratory
865.574.5131
caughmanjb@ornl.gov

ornl.gov

ORNL is managed by
UT-Battelle for the
US Department of Energy

OAK RIDGE National Laboratory

U.S. DEPARTMENT OF ENERGY

Fig. 37. Fact sheet for Laboratory C-101 in Building 5800.